

# Deep-Learning-aided Detection for Reconfigurable Intelligent Surfaces

Saud Khan, *Student Member, IEEE* and Soo Young Shin, *Senior Member, IEEE*

**Abstract**—This paper presents a deep learning (DL) approach for estimating and detecting symbols in signals transmitted through reconfigurable intelligent surfaces (RIS). The proposed network utilizes fully connected layers to estimate channels and phase angles from a reflected signal received through an RIS. Because the proposed network can estimate and detect symbols without any pilot signaling, this method reduces the overhead required for transmission. The improvements achieved by this method are quantified in terms of the bit-error rate, outperforming traditional detectors.

**Index Terms**—Deep learning, reconfigurable intelligent surface, estimation, detection

## I. INTRODUCTION

NEXT-GENERATION mobile communications networks have begun to be deployed, and compatible handsets will soon be available. The flexibility of wireless communications systems will be improved through the use of unconventional techniques, such as millimeter-wave communications, massive multiple-input multiple-output (MIMO) architectures, and network densification. However, these technologies often cannot be utilized to their full extent, because of their high power consumption and poor propagation in harsh environments. These limitations can be mitigated by modifying harsh propagation environments [1].

Recently, researchers have proposed controlling the channel medium by converting the environment space into a reconfigurable space, known as a reconfigurable intelligent surface (RIS). RIS environments are based on small, low-cost passive elements stacked together in the form of intelligent metasurfaces, which reflect incoming signals towards the receiver with a controllable phase shift. Unlike massive MIMO, RISs are based on a software-defined paradigm, and so they do not require any radio frequency (RF) processing, beamforming, relaying, or other physical RF solutions [2].

A key feature of RIS-assisted communications making them useful in smart radio environments is their relatively simple implementation, with inexpensive passive elements. However, this feature limits the estimation of channels and phase angles at the receiver end, because RISs cannot perform any RF processing. Therefore, to make RISs as passive as possible to minimize costs, the receiver must estimate the channel and received phase angle with minimal reliance on the RIS [3].

Deep learning (DL) approaches utilizing deep neural networks (DNNs) have been successfully applied in various fields,

such as computer vision and natural language processing. DL has been used for almost every aspect in communications frameworks, in both the physical and network layers, including power allocation [4] and channel estimation [5]. Recently, DL was applied to configure the optimal phase angles of RIS meta-elements in indoor communication environments [6]. However, that work assumes that some meta-elements of the RIS are active elements, used for channel estimation, which, reduces the passive nature of RIS. Furthermore, a complexity analysis of the proposed network and its adaptability in a complete channel mismatch scenario is also lacking since a perfect channel state information (CSI) was considered only.

Most existing studies have not explicitly focused on scenarios with imperfect CSI, or on reducing the complexities of the proposed networks. In the recent literature, very few studies have investigated the potential for applying DL to estimation and detection in an RIS-assisted communications system. The discussion below investigates this question and explicitly addresses the complexity of the DNN.

The present study makes the following contributions:

- We present a novel DL-based detector, called DeepRIS, for use in wireless receivers in RIS-assisted communications scenarios. DeepRIS estimates the channel fading and phase angles from the received signal.
- We explain the details of the implementation of the network, including the numbers of hidden and activation layers, number of neurons, and learning rate. Furthermore, the system-level integration of the proposed network in an RIS-empowered wireless communications scenario is discussed in detail.
- The complexity of the proposed DeepRIS detector is discussed in detail.
- Finally, simulation results are presented in terms of the bit-error rate (BER) in both perfect and imperfect CSI cases, and in scenarios in which the channels and reflecting elements are not matched. The results indicate that DeepRIS achieves a near-optimal BER.

## II. TRANSMISSION THROUGH RIS: SYSTEM MODEL

In this section, we provide an overview of the generic model of an RIS-assisted MISO communications system. As shown in Fig. 1, we consider a source ( $S$ ) equipped with  $M$  antennas communicating with the RIS comprised of  $N$  nearly passive elements, which, are reconfigurable and controlled using communication-oriented software. The RIS assists the communication by deliberately reflecting the signal from  $S$  towards the single-antenna destination  $D$  using low resolution phase shifters, owing to unfavorable propagation conditions.

The authors are with the WENS Lab, Department of IT Convergence Engineering, Kumoh National Institute of Technology, Republic of Korea (Email: saud.khan@ieee.org, wdragon@kumoh.ac.kr)

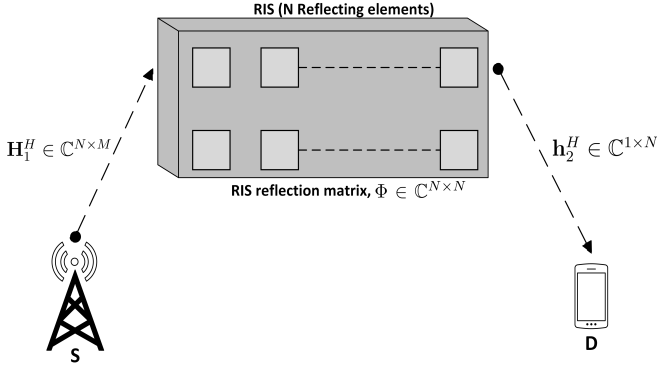


Fig. 1: Transmission through an RIS in a dual-hop communication scenario with no line-of-sight path between S and D.

Denoting the modulated signal transmitted by  $S$  as  $\mathbf{x} \in \mathbb{C}^{M \times 1}$ , the received downlink signal reflected through the RIS at  $D$  can be expressed as,

$$\mathbf{y} = (\mathbf{h}_2^H \Phi \mathbf{H}_1^H) \mathbf{x} + n \quad (1)$$

where  $\mathbf{H}_1^H \in \mathbb{C}^{N \times M}$  denotes the channel matrix from  $S$  to RIS,  $\mathbf{h}_2^H \in \mathbb{C}^{1 \times N}$  denotes the channel vector between the RIS and  $D$ .  $\Phi = \text{diag}[\phi_1, \phi_2, \dots, \phi_i]$  is a diagonal matrix representing the adjustable phase angle induced by the  $i_{th}$  reflector of the RIS, where  $\phi_i = e^{j\phi_i}$  and  $n \sim \mathcal{CN}(0, \sigma^2)$  represents additive white Gaussian noise (AWGN) [2].

Considering a single channel instance,  $\mathbf{H}_1^H = \alpha_i e^{-j\theta_i}$  and  $\mathbf{h}_2^H = \beta_i e^{-j\psi_i}$ , where  $\alpha_i, \beta_i \in [0, 1]$  and  $\theta_i, \psi_i \in [0, 2\pi]$  represents the channel amplitude and phase respectively. From (1), the instantaneous signal-noise ratio (SNR) at  $D$  is calculated as

$$\gamma = \frac{|\alpha_i \beta_i e^{j(\phi_i - \theta_i - \psi_i)}|^2 E_s}{N_0}, \quad (2)$$

where  $E_s$  represents the average energy per  $M$ -ary symbol. From (2), it follows that  $\gamma$  can be maximized when  $\phi_i = \theta_i + \psi_i$  for  $i = 1, \dots, N$ . In other words, the destination  $D$  will have the maximum received SNR when the phase angles from the reflecting elements of the RIS are known at  $D$ . Consequently, when the incoming channel phases are known at  $D$ , the maximum instantaneous received SNR can be expressed as

$$\gamma = \frac{(\alpha_i \beta_i)^2 E_s}{N_0} = \frac{A^2 E_s}{N_0}. \quad (3)$$

Noting that  $\alpha_i$  and  $\beta_i$  are independently Rayleigh distributed random variables, such that  $E[\alpha_i \beta_i] = \frac{\pi}{4}$  and  $\text{VAR}[\alpha_i \beta_i] = 1 - \frac{\pi}{16}$  for a large number of reflecting elements  $N \gg 1$ , it follows from the central limit theorem that  $A$  follows a Gaussian distribution with the parameters  $E[A] = \frac{N\pi}{4}$  and  $\text{VAR}[A] = N \left(1 - \frac{\pi^2}{16}\right)$  [1]. On the other hand, in case that the incoming phase angles  $\theta_i$  and  $\psi_i$  are unknown at  $D$ , the maximum instantaneous received SNR remains as in (2). From (2) and (3), one can infer that the receiver can only take full advantage of the reflecting elements of the RIS if the incoming phase angles are known. If the incoming phase angles are

unknown, then the gain is reduced as the number of reflecting elements in the RIS increases.

### III. PROPOSED DEEP LEARNING DETECTOR

This section details how DeepRIS can be implemented in an RIS-assisted communication scenario. As shown in Fig. 1, the scenario involves two-way channel fading and mismatched incoming phase angles. These challenges are addressed by the DeepRIS DNN, which is trained and then deployed at  $D$  to estimate the received signal without the need for channel estimation. The subsections below detail our analysis of the structure, function, training procedure, and online deployment of the proposed DeepRIS detector.

#### A. Structure of DeepRIS

DNNs consist of  $\ell$  layers having multiple neurons in every layer. The output of the network is a cascade of the nonlinear transformation of input data  $\mathbf{I}$  through all the previous layers, which is carried out iteratively. A fully connected layer means that neurons in a layer are connected with all the other neurons of the next layer. The output of such a network can be expressed as,

$$\mathbf{o} = f(\mathbf{I}, \Theta) = f^{(\ell-1)}(f^{(\ell-2)}(\dots f^{(1)}(\mathbf{I}))) \quad (4)$$

where,

$$f_i = \sigma(w_i \mathbf{I} + b_i)$$

here, each layer at its output has an activation function  $\sigma(\cdot)$  and corresponding weights  $w_i$  to the input data  $\mathbf{I}$  at every training iteration. An additional bias term  $b$  is also added to balance the sparse weight balancing during training.

The proposed DeepRIS network consists of four hidden layers, each of which is fully connected layer followed by a hyperbolic tangent (tanh) activation function with the range  $[-z, z]$ . The tanh activation function is preferred over the rectified linear activation function (ReLU) because tanh keeps the negative weights from previous layers intact, whereas ReLU reduces all negative weights to zero. The tanh and ReLU functions can be formally defined as

$$\begin{aligned} \sigma_{\text{tanh}}(z) &= \frac{\sinh(z)}{\cosh(z)} \\ &= \frac{e^z - e^{-z}}{e^z + e^{-z}} \end{aligned} \quad (5)$$

$$\sigma_{\text{ReLU}}(z) = \max(0, z),$$

where  $z$  denotes the range of the amplitude of the adopted modulation scheme. One can infer that the tanh function allows the negative weights to persist, whereas the ReLU function reduces all negative weights to zero. This is important to note, because the incoming phase angles and the fading channels will also affect the negative modulated constellation symbols. If ReLU is used as the activation function, then the negative constellation symbols will be reduced to zero, and the network will collapse during training. In contrast, the tanh activation function keeps the negative weights intact, facilitating the

---

**Algorithm 1** DeepRIS Training Algorithm
 

---

**Input:** Original transmitted symbols, channel and phase-affected symbols.

**Output:** Trained DeepRIS network.

- 1: Initialization: All parameters including weights, biases, and iterations are set to 0. The validation error threshold is set to  $k$ .
  - 2: Produce a set of training patches  $\Psi$ .
  - 3: Process the training patches with simulated channel distortions and phase angles according to Eq. (1).
  - 4: **while** ( $k \leq \mathcal{L}$ ) Train the DNN by minimizing the loss function according to Eq. (6).
  - 5:     Update  $\mathcal{L}(\Theta)$  according to Eq. (7) and (8).
  - 6: **end while**
  - 7: **return:** DeepRIS network
- 

training process such that the DNN can accurately estimate the incoming channel and phase angles.

The fully connected layers are designed with the aim that the network can successfully decode the received channel-impaired reflected signals from the RIS with unknown phase angles. This objective is complicated by dual-channel fading from  $S$  to the RIS and from the RIS to  $D$ , as well as unknown phase angles. Therefore, the number of layers and number of neurons in each layer must be correctly identified. Furthermore, the complexity of the network must be kept at a minimum. Consequently, following a test and trial method, the numbers of neurons in the fully connected layers are set to 500, 250, 100, and 7, in sequence.

### B. Model Training

Before DeepRIS can be deployed as a detector, the model needs to be trained offline with a wide range of instances of channels and phase variances. Random data sequences of bit length  $b$  from the source  $S$  are generated to simulate transmission vectors. These vectors are then transmitted towards the  $N$  reflecting elements of the RIS, and the signal is subject to channel fading  $\mathbf{H}_1^H$ . The vectors directed towards the RIS are reflected towards the destination  $D$  with phase angles  $\Phi$ , and are again subject to channel fading  $\mathbf{h}_2^H$  along this path. Consequently, the received signal at the destination  $D$  is affected by dual-channel fading, and by the phase angles of the  $N$  reflector elements of the RIS.

The received channel-faded vectors  $\mathbf{y}$  and original transmitted vectors  $\mathbf{x}$  are arranged in a training sequence. Because the objective of the DeepRIS model is to estimate the original transmitted symbols at destination  $D$ , the model is trained with the objective of minimizing the difference between the received vector  $\mathbf{y}$  and the original transmitted vector  $\mathbf{x}$ . Therefore, the loss function for the DeepRIS model is defined as

$$\begin{aligned} \mathcal{L}(\Theta) &= \frac{1}{N} \sum_k \|\mathbf{y}(\mathbf{k}) - \mathbf{x}(\mathbf{k})\|_2^2 \\ &= \frac{1}{N} \sum_k \left\| \underbrace{[\mathbf{h}_2^H \Phi^H \mathbf{H}_1^H] \mathbf{x}(\mathbf{k}) + n}_{\xi} \right\|_2^2, \end{aligned} \quad (6)$$

TABLE I: Parameters used for simulations

Parameter	Value
Input layer dimension	14
Modulation scheme	4-QAM
Transmit antennas, $M$	32
Reflecting elements, $N$	64
Channel fading	$\mathbf{H}_1^H, \mathbf{h}_2^H \sim \mathcal{CN}(0, 1)$
Pathloss	$\frac{10^{-2}}{d^{-3.75}}; d = 2$
AWGN	$n \sim \mathcal{CN}(0, SNR)$
SNR during training	0dB - 30dB
Batch size	64
No. of training data samples	$7 \times 10^4$
Validation split	20%
Validation patience	50
Total training steps	1000
Optimizer	Adam, $\delta_1 = 0.9, \delta_2 = 0.999$
Learning rate, $\eta$	0.01

where the objective is to estimate  $\xi$  over  $k$  iterations. This process yields a generic formulation for the estimation of the channel and phase angles in the hidden layers of DeepRIS at the  $k_{th}$  iteration. Moreover,  $\Theta$  represents the weights and biases of the DeepRIS model, which are updated at every iteration. The parameters  $\Theta$  are updated using the Adam optimizer, which is defined as

$$\Theta_{\ell+1} = \Theta_{\ell} - \frac{\eta m_{\ell}}{\sqrt{v_{\ell} + \epsilon}}, \quad (7)$$

where  $\eta$  is the learning rate with which the optimizer defines the step size, and  $\epsilon$  is a smoothing term that prevents division by zero. Furthermore,  $m_{\ell}$  and  $v_{\ell}$  are estimates of the mean and uncentered variance of the gradients, respectively, defined as

$$\begin{aligned} m_{\ell} &= \delta_1 m_{\ell-1} + (1 - \delta_1) \nabla \mathcal{L}(\Theta_{\ell}) \\ v_{\ell} &= \delta_2 v_{\ell-1} + (1 - \delta_2) \nabla [\mathcal{L}(\Theta_{\ell})]^2, \end{aligned} \quad (8)$$

where  $\delta_1$  and  $\delta_2$  are the decay rates of the moving average. If the gradients in (8) are similar over many iterations, then the moving average helps the gradients to gain momentum in a certain direction. Conversely, if the gradients are highly noisy because of sparse training data, then the moving average of the gradient is smaller, and so the parameter updates are also smaller. This relationship is essential in the present case, because the inputs to the DeepRIS detector will be contaminated by both dual-channel fading and the effects of mismatched phase angles. Therefore, by generating a large and diverse training dataset and training the DNN using the Adam optimizer, the DeepRIS detector can converge towards an optimal solution to the problem at hand.

A training mechanism is implemented for DeepRIS to be effectively trained. First, the network is initialized with empty matrices of weights and biases. Next, random data sequences of size  $\Psi$  are generated and affected using different channel and AWGN intensities and reflected through different  $N$  reflector elements of the RIS. These sequences are subsequently used to train the DeepRIS in an unsupervised manner, where the estimated received signal at the output of the network is updated at every iteration. The concrete learning paradigm is also described in Algorithm 1. By shuffling the channel and AWGN intensities at each iteration, the network maps

the effects of the channel and phase angles on the transmitted signal using the nonlinear function approximation in its hidden layers, which help to avoid overfitting of the network.

#### IV. SIMULATION RESULTS

Simulation results are used to verify the DeepRIS detector's performance in terms of the BER. DeepRIS yields an improved performance compared with the conventional least squares (LS) and minimum mean square error (MMSE) estimators. We also discuss the computational complexity of the proposed DeepRIS network during training and deployment, in terms of big- $\mathcal{O}$  notation. For simulations, we consider a composite channel fading based of Rayleigh fading and pathloss component of 3.75 with distance  $d = 2$  from the RIS to destination  $D$ . During training, we use 20% of the training data as validation test set to the DeepRIS network and set the validation patience to 50 iterations. This essentially means if the training and validation error is linear for 50 iterations, the network will stop the training process. This is an important step in the training process as it greatly helps in avoiding overfitting of the network on the training data. We use MATLAB for our simulations, and the system parameters used during these simulations are listed in Table I.

##### A. BER Analysis

We extensively evaluate the BER performance and test various mismatch scenarios to investigate the redundancy of DeepRIS in different situations. Fig. 2 (a) plots the BER curves of DeepRIS and conventional schemes when full CSI is available. As shown, DeepRIS outperforms both state-of-the-art MMSE and LS methods, and is comparable to the optimal ML detector. The improved performance of DeepRIS is mainly attributed to the deep architecture of the network, and the extensive training process that helps DeepRIS to regularize to generic variances in channels and phase angles.

In Fig. 2 (b), the BER performance of DeepRIS is plotted when only imperfect CSI is available, and compared with those of traditional detection schemes. Imperfect CSI means that the receiver is unaware of the channel fading and the receiving phase angles from the RIS. In this case, the transmission is blind. These results show that DeepRIS performs well in situations for which it was not trained. It also outperforms conventional schemes, and performs on the level of ML detection. These findings show that DeepRIS is well suited to generic scenarios, and can be deployed without retraining. Moreover, it shows that DL-based detectors can estimate the channel and phase angles of the received signals without explicitly relying on pilot signal-based estimation, which is an important issue in RIS-assisted wireless communications.

Next, we discuss rigorous performance tests of DeepRIS in situations for which the network was not trained. Although the network is trained using training samples with simulated channel statistics, it is essential that the network performs robustly in the case of unforeseen channel fading. Therefore, a channel mismatch scenario was simulated using Nakagami- $m$  fading, to analyze how this fading affects the performance of DeepRIS. Nakagami- $m$  fading describes small-scale fading

effects, and has two parameters that define its shape  $m$  and spread  $\Omega$ . Fig. 2 (c) plots the effects of different channel conditions on DeepRIS in terms of the fading strength  $m = 1$  and spreading factor  $\Omega = 2$ . Furthermore, Fig. 2 (d) analyzes the performance of DeepRIS in the additional untrained scenario in which the number of reflecting elements  $N$  of the RIS varies. The results show that the variations in the channel or number of reflecting elements do not significantly degrade the performance of DeepRIS, proving that the network is generalizable.

##### B. Complexity Analysis

This section analyzes the computational complexity of DeepRIS. The complexity analysis is conducted by calculating the number of operations at each fully connected layer using Big- $\mathcal{O}$  notation. Ignoring the input layer,  $p, q, r,$  and  $s$  denote the numbers of nodes in the first, second, third, and fourth hidden layers, respectively. We represent the weights for moving from one layer to another in the form of the matrices  $W_{qp}, W_{rq},$  and  $W_{sr},$  respectively, where  $q, p,$  and  $s$  on represent the rows and columns of each weight matrix. The time complexities of operations at every layer are defined as follows:

- Time complexity from dense layer 1  $\rightarrow$  2:  $\mathcal{O}(q * p)$
- Time complexity from activation layer 1  $\rightarrow$  2:  $\mathcal{O}(q)$
- Time complexity from dense layer 2  $\rightarrow$  3:  $\mathcal{O}(r * q)$
- Time complexity from activation layer 2  $\rightarrow$  3:  $\mathcal{O}(r)$
- Time complexity from dense layer 3  $\rightarrow$  4:  $\mathcal{O}(s * r)$
- Time complexity from activation layer 3  $\rightarrow$  4:  $\mathcal{O}(s)$
- Time complexity of number of iterations:  $\mathcal{O}(k)$
- Time complexity of number of training samples:  $\mathcal{O}(t)$

Assuming that  $t$  training samples pass from Layer 1 to 2 through activation layer 1, we see that

$$\begin{aligned} &\mathcal{O}(q * p * t + q * t) \\ &\mathcal{O}(q * p * (t + 1)) \\ &\mathcal{O}(q * p * t). \end{aligned} \quad (9)$$

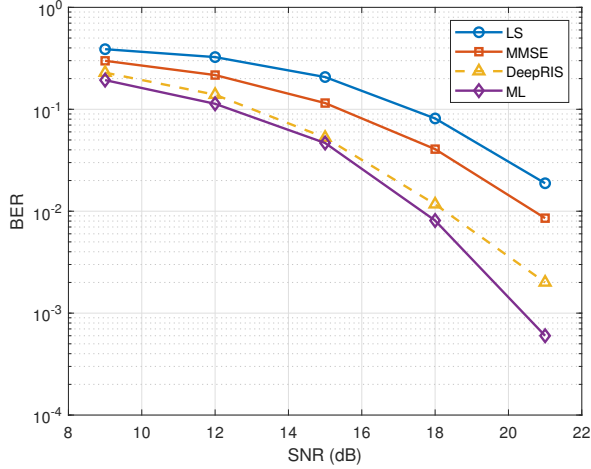
Using the same logic for the movements from  $q \rightarrow r$  and  $r \rightarrow s$ , the time complexity for DeepRIS during training will be

$$\mathcal{O}(k * t * (qp + rq + sr)). \quad (10)$$

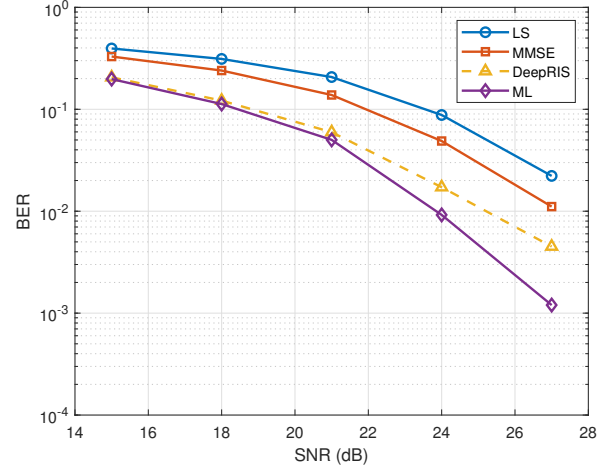
The complexity of a network is different during the training and testing stages. During training, a network is trained over many iterations so that it can be generalized and resilient against overfitting of the data. Hence, the training complexity is the network complexity times the number of iterations  $k$ , as shown in Eq. (10). However, during testing and deployment each input to the network is only passed through the network once, with a decision at the output layer. Thus, after training Eq. (10) reduces to

$$\mathcal{O}(qp + rq + sr), \quad (11)$$

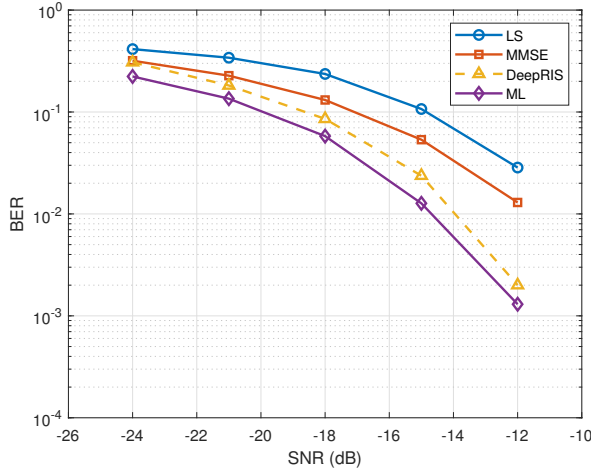
which is the final computational complexity of the deployed DeepRIS network. In comparison with ML detection and MMSE, which have computational complexities of  $\mathcal{O}(2^k)$  and  $\mathcal{O}(k^3)$ , respectively, the proposed DeepRIS detector offers a superior performance with a lower complexity.



(a) DeepRIS and traditional methods under perfect CSI.



(b) DeepRIS and traditional methods under imperfect CSI.



(c) DeepRIS in channel mismatch scenario.

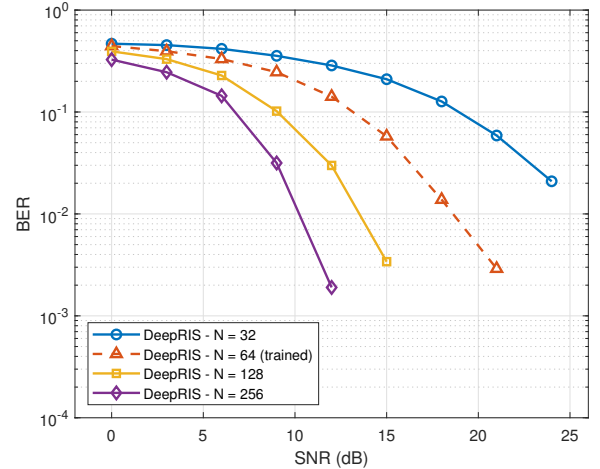
(d) DeepRIS in  $N$  reflecting elements mismatch scenario.

Fig. 2: BER Performance of DeepRIS in RIS-assisted communications system.

## V. CONCLUSION

This work has demonstrated the usefulness of DL methods for estimating channels and phase angles in RIS-assisted wireless communication systems. The DeepRIS detector achieves a strong performance in terms of the BER. The model is first trained offline using simulated channel and phase instances. Then, the trained DeepRIS model is deployed to estimate channels and phase angles from the received symbols. The network is easy to train and adaptive to dynamic channel conditions, while achieving a lower BER than conventional schemes.

To prepare the model for practical deployment, it must be further generalized to avoid overfitting and perform efficiently in scenarios in which channels and phases are mismatched. The preliminary results presented here confirm the potential of DL for estimating channels and phase angles in RIS-assisted wireless communication systems.

## REFERENCES

[1] E. Basar, "Transmission through large intelligent surfaces: A new frontier in wireless communications," in *2019 European Conference on Networks*

and Communications (*EuCNC*), June 2019, pp. 112–117.

[2] Q.-U.-A. Nadeem, A. Kammoun, A. Chaaban, M. Debbah, and M.-S. Alouini, "Intelligent reflecting surface assisted multi-user miso communication," *arXiv preprint arXiv:1906.02360*, 2019.

[3] M. Di Renzo, M. Debbah, D.-T. Phan-Huy, A. Zappone, M.-S. Alouini, C. Yuen, V. Sciancalepore, G. C. Alexandropoulos, J. Hoydis, H. Gacanin *et al.*, "Smart radio environments empowered by reconfigurable ai metasurfaces: an idea whose time has come," *EURASIP Journal on Wireless Communications and Networking*, vol. 2019, no. 1, p. 129, 2019.

[4] S. Khan, K. S. Khan, and S. Y. Shin, "Symbol denoising in high order m-qam using residual learning of deep cnn," in *2019 16th IEEE Annual Consumer Communications & Networking Conference (CCNC)*. IEEE, 2019, pp. 1–6.

[5] S. Khan and S. Y. Shin, "Deep learning aided transmit power estimation in mobile communication system," *IEEE Communications Letters*, vol. 23, no. 8, pp. 1405–1408, 2019.

[6] C. Huang, G. C. Alexandropoulos, C. Yuen, and M. Debbah, "Indoor signal focusing with deep learning designed reconfigurable intelligent surfaces," in *2019 IEEE 20th International Workshop on Signal Processing Advances in Wireless Communications (SPAWC)*, July 2019, pp. 1–5.